Steady state modeling of desiccant wheels

Bellemo, Lorenzo; Elmegaard, Brian; Kærn, Martin Ryhl; Markussen, Wiebke Brix; Reinholdt, Lars O.

Published in:
Proceedings of the International Sorption Heat Pump Conference (ISHPC) 2014

Publication date:
2014

Steady state modeling of desiccant wheels

Lorenzo Bellemo[1]*, Brian Elmegaard[1], Martin R. Kærn[1], Wiebke B. Markussen[1], Lars O. Reinholdt[2]

[1]Technical University of Denmark, Mechanical Engineering Department, Thermal Energy Section, Kgs. Lyngby 2800, Denmark

[2]Danish Technological Institute, Energy and Climate Division, Refrigeration and Heat Pump Technology, Aarhus 8000, Denmark

* Corresponding Author
lobel@mek.dtu.dk

ABSTRACT

Desiccant wheels are rotary desiccant dehumidifiers used in air conditioning and drying applications. The modeling of simultaneous heat and mass transfer in these components is crucial for estimating their performances, as well as for simulating and optimizing their implementation in complete systems. A steady state two-dimensional model is formulated and implemented aiming to obtain good accuracy and short computational times. Comparison with experimental data from the literature shows that the model reproduces the physical behavior of desiccant wheels. Mass diffusion in the desiccant should be taken into account in a future version of the model. More experimental data have to be gathered to implement eventual missing phenomena and validate the model for all input parameters.

1. INTRODUCTION

Desiccant Wheels (DWs) are mainly used in drying applications as well as in desiccant cooling systems for air conditioning (La et al., 2010). DWs are constituted by identical channels aligned lengthwise and distributed into concentric layers. This structure is obtained by means of a support material onto which the desiccant is attached. The wheel is divided into two sections, namely process and regeneration sections. The process airstream, to be dehumidified, flows through the process section, while the regeneration airstream flows through the regeneration section from the opposite direction. A small electric motor makes the wheel rotating, i.e. all channels move continuously between the two sections. A sketch of the considered DW configuration is reported in Fig. 1, including a detailed front view of a sinusoidal channel.

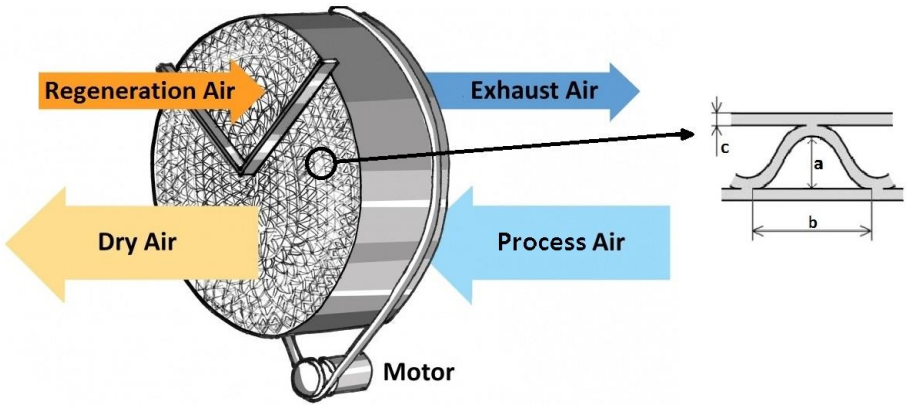

Figure 1. Desiccant wheel sketch and detailed front view of a sinusoidal channel

The dehumidification mechanism taking place in the process section is adsorption: water vapor molecules migrate from the humid air to the desiccant and diffuse inside the desiccant capillaries, where they remain bounded on the desiccant surface. The adsorption process is exothermic, resulting in an increased temperature of the dried air. In the regeneration section the opposite phenomenon, termed desorption, takes place by circulating a hot airstream with low relative humidity. Adsorption and desorption are driven by the water vapor partial pressure difference between the bulk of humid air and the layer of humid air at the desiccant surface. The wheel rotation allows for a continuous dehumidification process and enables to reach steady state operation, i.e. the air outlet conditions are constant over time when the air inlet conditions and rotational speed are kept constant.

Several DW models have been developed in the last decades. Disregarding empirical models, two different approaches for modeling of coupled heat and mass transfer processes taking place in a DW can be identified.

The most common approach considers a single channel in the DW, i.e. a control mass of desiccant with a varying inlet airflow according to the angular position. The desiccant control mass experiences varying conditions due to the rotation of the wheel. The corresponding system of partial differential equations for calculating the desiccant and air conditions is solved over time: to obtain a steady state operating condition the differential equations are solved by numerical integration. The conditions at different DW circumferential locations correspond to the conditions at different time steps for the control mass of one channel. A review of models based on this approach is presented in (Ge et al., 2008).

Another approach consists of dividing the entire DW into control volumes similarly to thermodynamic cycles. Flows of both air and desiccant enter and exit each control volume. To find a steady state solution, the corresponding mathematical model consists of a system of algebraic equations expressing energy and mass balances and heat and mass transfers. This approach reduces the computational effort required to solve the system, i.e. DW steady state operation can be quickly computed, facilitating the simulation of more complex systems. Two previous studies based on this approach are reported in (Tsutsui, 2008) and (Harshe, 2005).

The model presented in this paper is based on the control volume approach, aiming to obtain good accuracy and short computational time to also facilitate whole system simulations.

2. METHODS

2.1 Model formulation

The DW model is based on a control volume approach: the computed air and desiccant flow conditions to and from a control volume as well as the conditions in a control volume are constant in time during steady state operation. The discretization approach is illustrated in Fig. 2, while the resulting 2D computational grid is shown in Fig. 3 considering N_x control volumes in the axial direction and N_ϑ control volumes in the circumferential direction.

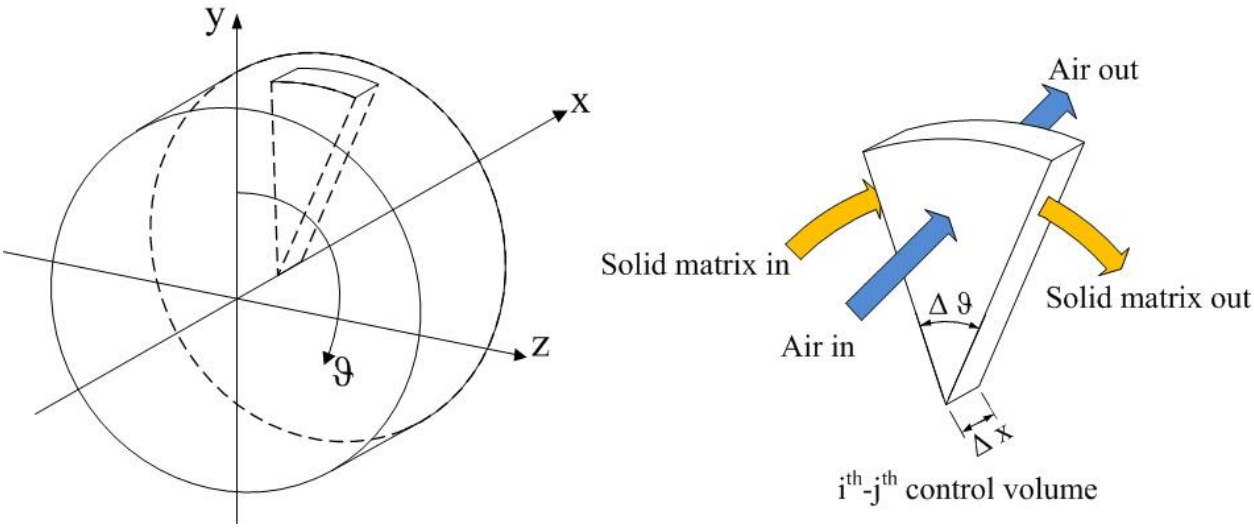

Figure 2. 2D Control volume discretization approach

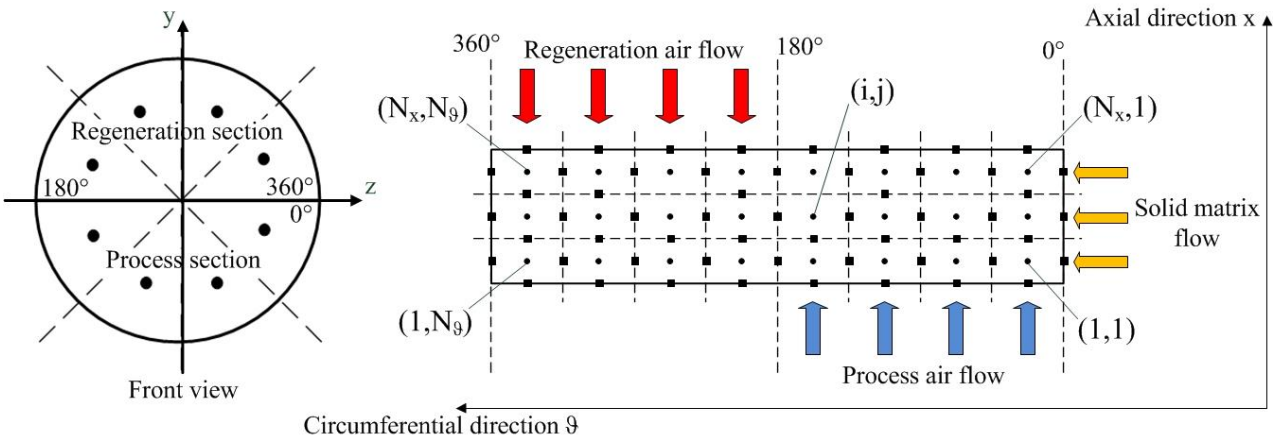

Figure 3. 2D DW computational grid with 180° regeneration angle

The inputs to the model are:

- DW geometrical characteristics (diameter, length, regeneration angle).
- Channel geometrical characteristics (*a*, *b*, *c* in Fig. 1).
- DW rotational speed.
- Desiccant material characteristics (density, specific heat, adsorption isotherm, heat of adsorption).
- Air inlet conditions (temperatures, humidity contents, volume flow rates).

The model is based on the following assumptions:

1) The wheel does not exchange heat with the surroundings.
2) All channels are identical, i.e. airflows are homogeneously distributed among the channels at both sides.
3) The desiccant material is uniformly distributed on the support structure.
4) No heat and mass transfer take place between adjacent channels.
5) All of the generated adsorption/desorption heat is delivered to/extracted from the desiccant.
6) Air velocity is much higher than wheel rotational speed, i.e. air enters and exits the same control volume.
7) Air and desiccant are in equilibrium at the desiccant surface.
8) Axial and radial heat conduction and mass diffusion are neglected both in the air and in the desiccant.
9) Variations of temperatures and humidity contents along the DW radial direction are neglected.
10) In each control volume the spatial gradient of air and desiccant conditions is null.
11) Condensation of water on the desiccant surface in the regeneration side is not considered.

Under these assumptions the energy and mass balances are written for the generic (i,j) control volume.
The mass balance applied to dry air provides:

$$\dot{m}_{a,in} = \dot{m}_{a,out} = \dot{m}_a \tag{1}$$

The mass balance applied to dry solid matrix provides:

$$\dot{m}_{m,in} = \dot{m}_{m,out} = \dot{m}_m \tag{2}$$

The mass balance applied to water is expressed as:

$$\dot{m}_a\left(\omega_{in(i,j)} - \omega_{out(i,j)}\right) + \dot{m}_m\left(W_{in(i,j)} - W_{out(i,j)}\right) = 0 \tag{3}$$

The energy balance applied to humid air is expressed as:

$$\dot{m}_a\left(I_{ha,in(i,j)} - I_{ha,out(i,j)}\right) + \dot{Q}_{sens(i,j)} + \dot{Q}_{lat(i,j)} = 0 \tag{4}$$

where the humid air specific enthalpy specific enthalpy for generic conditions is defined as:

$$I_{ha} = c_{p,a}T_a + \omega\left(c_{p,v}T_a + q_{vap,0°C}\right) \tag{5}$$

Heat transfer between humid air and solid matrix in Eq. (4) is indicated as the sum of a sensible contribution associated to convective heat transfer and a latent contribution associated to convective mass transfer:

$$\dot{Q}_{sens(i,j)} = h_{(i,j)}A\left(\overline{T}_{a(i,j)} - \overline{T}_{eq(i,j)}\right) \tag{6}$$

$$\dot{Q}_{lat(i,j)} = \dot{m}_{w(i,j)}\, q_{vap(i,j)} \tag{7}$$

where the overlined terms are central difference averages in the control volume. The latent heat exchanged by the air is directly proportional to the latent heat of vaporization of water and not to the heat of adsorption, as it is assumed the generated heat of adsorption is exchanged with the desiccant.
The mass flow rate of water adsorbed or desorbed in a control volume is calculated as:

$$\dot{m}_{w(i,j)} = \sigma_{(i,j)}A\left(\overline{\omega}_{(i,j)} - \overline{\omega}_{eq(i,j)}\right) = \dot{m}_a\left(\omega_{in(i,j)} - \omega_{out(i,j)}\right) \tag{8}$$

The desiccant adsorption isotherm couples the water content in the desiccant with the relative humidity of adjacent air in thermal equilibrium with the desiccant, which allows computing mass transfer between air and desiccant.
The energy balance applied to the entire control volume is expressed as:

$$\dot{m}_a\left(I_{ha,in(i,j)} - I_{ha,out(i,j)}\right) + \dot{m}_m\left(I_{wm,in(i,j)} - I_{wm,out(i,j)}\right) - \dot{m}_{w(i,j)}\left(q_{ads(i,j)} - q_{vap(i,j)}\right) = 0 \tag{9}$$

where the wet solid matrix (including water) specific enthalpy for generic conditions is defined as:

$$I_{wm} = \left(c_{p,m} + Wc_{p,w}\right)T_m \tag{10}$$

The humid air specific enthalpy in Eq. (5) takes into account the latent heat of vaporization of water and the wet solid matrix specific enthalpy in Eq. (10) takes into account water as being in the liquid state: the first two terms on the LHS of Eq. (9) consider water as being condensed and not adsorbed on the desiccant surface. The energy difference between the adsorbed and condensed states of the adsorbed amount of water is taken into account by including a correction term in the energy balance for the entire control volume, i.e. the third term on the LHS in Eq. (9), as also suggested in (Barlow, 1982). This corresponds to include a term in Eq. (9) accounting for the integral heat of wetting of the solid surface.
The combination of Eq. (4) and (9) result into the energy balance applied to solid matrix:

$$\dot{m}_m\left(I_{wm,in(i,j)} - I_{wm,out(i,j)}\right) - \dot{Q}_{sens(i,j)} - \dot{m}_{w(i,j)}\, q_{ads(i,j)} = 0 \tag{11}$$

showing the latent heat exchanged by the solid matrix is directly proportional to the heat of adsorption.
The airflow regime in the channels is laminar: Reynolds number is below 500 for generic air conditions, air velocities up to 5 m/s and typical channel hydraulic diameters (approx. 1.5 mm).
The Nusselt number for fully developed laminar flow in a sinusoidal channel only depends on the channel dimensions as reported in (De Antonellis et al., 2010), and it is calculated as a function of the channel aspect ratio (see Fig. 1):

$$Nu_{FD} = 1.1791 \cdot \left[1 + 2.7701 \cdot (a/b) - 3.1901 \cdot (a/b)^2 + 1.9975 \cdot (a/b)^3 - 0.4966 \cdot (a/b)^4\right] \tag{12}$$

The local Nusselt number along a channel is calculated taking into consideration the hydraulic and thermal airflow development (De Antonellis et al., 2010):

$$Nu_{(i,j)} = Nu_{FD} + \frac{0.0841}{0.002907 + [(D_h/x)\,\mathrm{Re}_{(i,j)}\,\mathrm{Pr}_{(i,j)}]^{-0.6504}} \tag{13}$$

where x [m] is the local position along the DW axis, set to zero at the channel entrance.
The analogy between heat and mass transfer states that Sherwood number can be calculated with the same correlation used for Nusselt number by substituting Prandtl number with Schmidt number (Mills, 2001):

$$\sigma_{(i,j)} = \frac{h_{(i,j)}}{c_{p,a} Le_{(i,j)}^{(1-n)}} \tag{14}$$

The exponent of Le in Eq. (9) contains n [-], which corresponds to the exponent of Prandtl number in the correlation for Nusselt number expressed in a form like $Nu=C \cdot Re^m \cdot Pr^n$.
In addition the model includes expressions for the adsorption isotherm and the heat of adsorption, which are introduced in the following for the considered desiccant material.

2.1 Model implementation

The model is implemented in Engineering Equation Solver (EES). A Central Difference Scheme (CDS) is adopted to compute all variables at the control volume centers. Both process and regeneration air outlet conditions, averaged for each section, are found to not change significantly by increasing the number of control volumes over 40 along the circumferential direction and 5 along the axial direction, i.e. 200 control volumes. The numerical method has been tested in the range of conditions reported in Table 1. For all tested conditions, the required computational time using 200 control volumes is within 10 seconds.

Table 1: Range of parameter values used for testing the DW model

Parameter	**Min/Max values**
Process side air inlet temperature [°C]	15-40
Regeneration temperature [°C]	50-90
Process and regeneration air inlet humidity ratio [g_v/kg_a]	9-20
Wheel rotational speed [rph]	5-80
Regeneration angle [°]	90-180
Wheel diameter [mm]	400-2000
Wheel length [mm]	20-400

3. RESULTS

3.1 Model validation

The mathematical model is implemented and simulated in Engineering Equation Solver (EES).
Experimental data from (Tsutsui, 2008) are used to verify the model by a sensitivity analysis on important inputs to the model. The measurements reported in (Tsutsui, 2008) are obtained with thermocouples with a precision of ± 0.05°C for temperatures and dew point sensors with precision of ± 0.2°C for dew points.
The dimensions of the sinusoidal channels are chosen to obtain a similar hydraulic diameter as in (Tsutsui, 2008), where a honeycombed structure was considered. The input dimensions are reported in Table 2.

Table 2: Reference DW characteristics

Parameter	**Value**
DW diameter	350 mm
DW length	50 mm
Channel hydraulic diameter	15.4 mm
Channel height	1.9 mm
Channel width	3.8 mm
Channel wall thickness	0.2 mm
Regeneration angle	180°

The considered desiccant material is Regular Density (RD) silica gel, whose properties are reported in Table 3.

Table 3: Desiccant material properties

Parameter	**Value**
Silica gel density	800 kg/m^3
Silica gel specific heat capacity	921 J/(kgK)

The RD silica gel adsorption isotherm is calculated neglecting the effect of temperature (Pesaran, 1980):

$$\phi_{eq} = 0.0078 - 0.0576 \cdot W + 24.17 \cdot W^2 - 124.48 \cdot W^3 + 204.23 \cdot W^4 \quad (15)$$

According to Eq. (15) the maximum water content in the desiccant is approximately 40% of its dry mass.
The heat of adsorption of RD silica gel is expressed as a function of the vaporization heat and the water content in the desiccant (Brandemuhel, 1982):

$$q_{ads} = q_{vap} \cdot \left(1 + 0.2843 \cdot e^{-10.28 \cdot W}\right) \quad (16)$$

Eq. (15) and (16) are used for both adsorption and desorption, i.e. the two processes have the same characteristics and the only difference is the direction of heat and mass transfer.
Simulations are carried out for varying regeneration temperatures T_{reg} (regeneration air inlet temperature), air face velocities, DW lengths, and wheel rotational speeds as shown in Fig. 4-5-6.
For all simulations, the reference airstream inlet conditions are:

- Process air face velocity 2 m/s, i.e. process airflow rate is approximately 350 m^3/h.
- Process and regeneration airflow rates are equal, i.e. air face velocities are approximately equal.
- Process air inlet conditions are 32.5°C and 19.5 g_v/kg_a.
- Regeneration air inlet conditions are 80°C and 11.9 g_v/kg_a.

In all simulations the exponent *n* in Eq. (14) is set equal to 1, which provides the same results as setting *Le*=1. Varying *n* in a range 0.2-1 does not have any significant impact on the results.

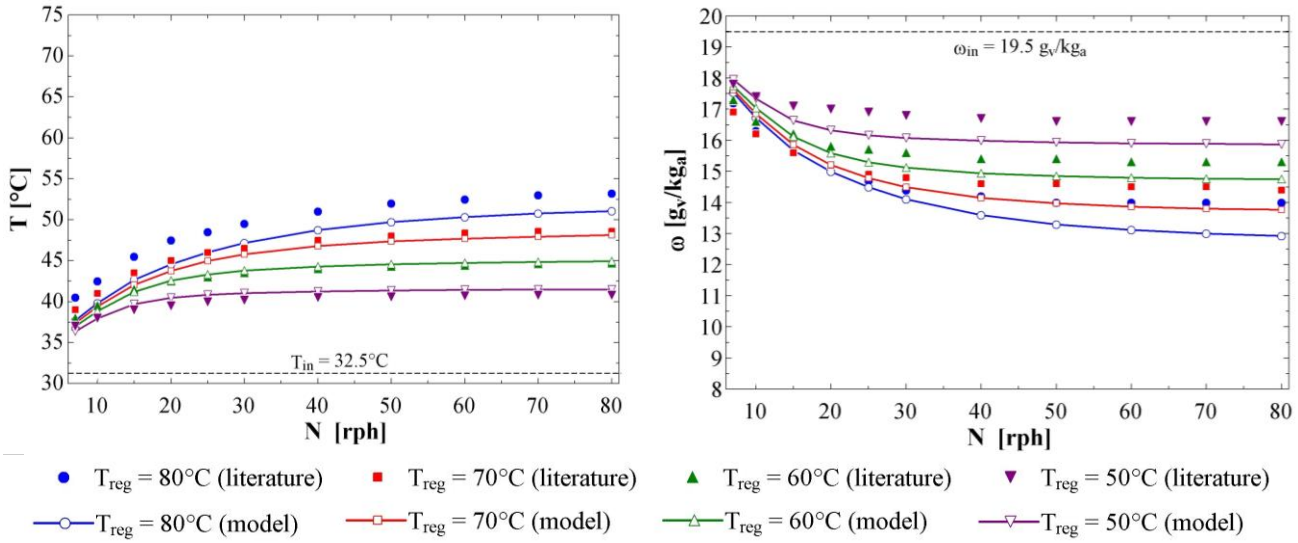

Figure 4. Process air outlet conditions for varying T_{reg} and N

Fig. 4 shows good agreement between the model and experimental data in terms of temperatures, while there are some differences in terms of humidity ratios, up to 1 g_v/kg_a for T_{reg}=80°C and high wheel rotational speed, for which also temperatures differ of approximately 4°C. It is noticed that in all cases the model underestimates dehumidification in comparison to experimental data at low rotational speeds and overestimates it as the rotational speed increases.

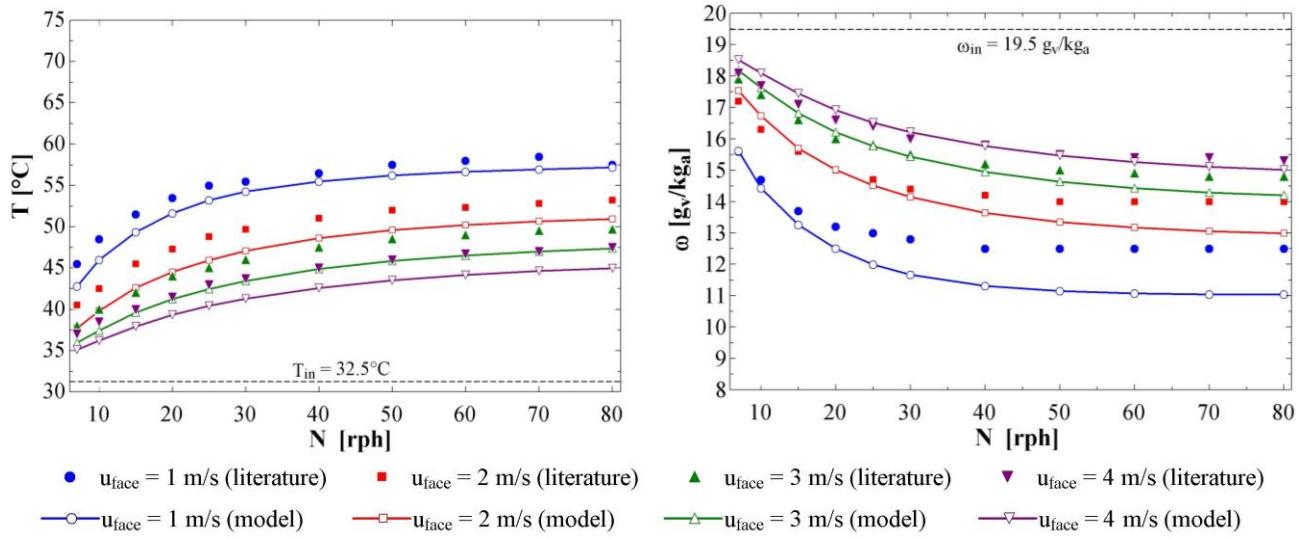

Figure 5. Process air outlet conditions for varying u_{face} and N

Fig. 5 shows again a better agreement between the model and experimental data in terms of temperatures than humidity ratios, which can differ up to 1.5 g_v/kg_a for u_{face}=1 m/s at high rotational speeds. The biggest discrepancies for temperatures are instead observed for the lowest u_{face}. Again dehumidification is underestimated by the model at low rotational speeds and overestimated at high rotational speeds.

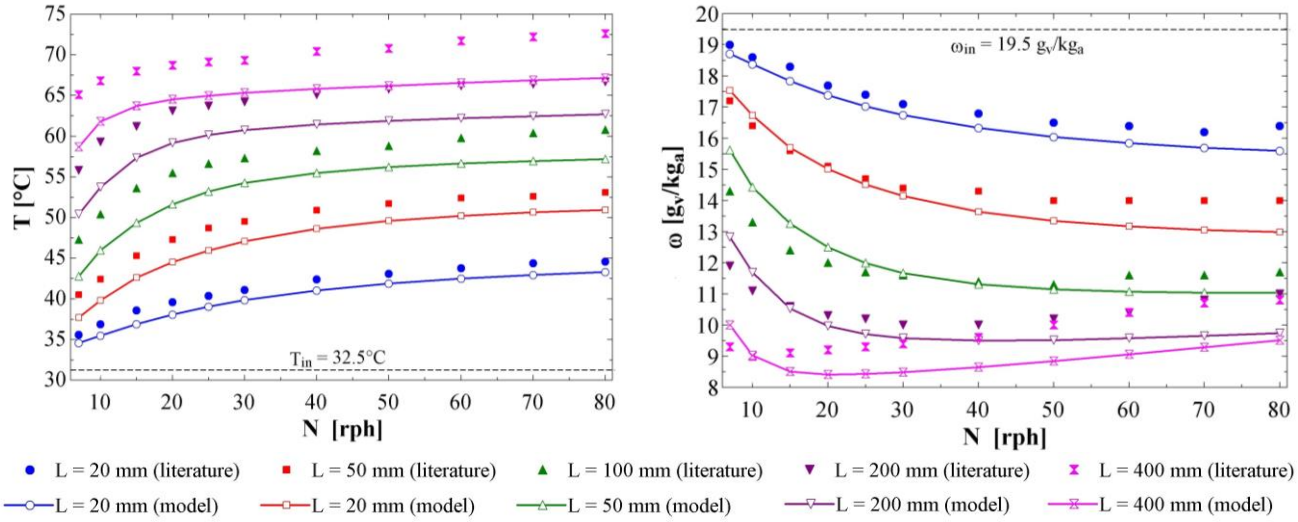

Figure 6. Process air outlet conditions for varying *L* and *N*

Fig. 6 shows the model provides the same variation trends as experimental data both for temperatures and humidity ratios. The computed humidity ratio for DW lengths of 200 and 400 mm become almost equal at high rotational speeds. The biggest differences between the computed values and experimental data are found for the longest DW at high rotational speeds, where the humidity ratio difference is 1.5 g_v/kg_a and temperature difference is 11°C. The air heating effect is always underestimated to different extents depending on the rotational speed, and the difference between the computed temperatures and experimental data is almost constant for the whole range of rotational speeds. Also in this case dehumidification is generally underestimated at low rotational speeds and overestimated at high rotational speeds.

Solving the reference case with 40 circumferential control volumes and 5 axial control volumes, the parameter affecting computational time the most is the wheel rotational speed: computational time increases for increasing rotational speeds, i.e. higher mass flow rates of the solid matrix flowing through each control volume.

The air outlet conditions along the circumferential direction at both DW sides are reported in Fig. 7.

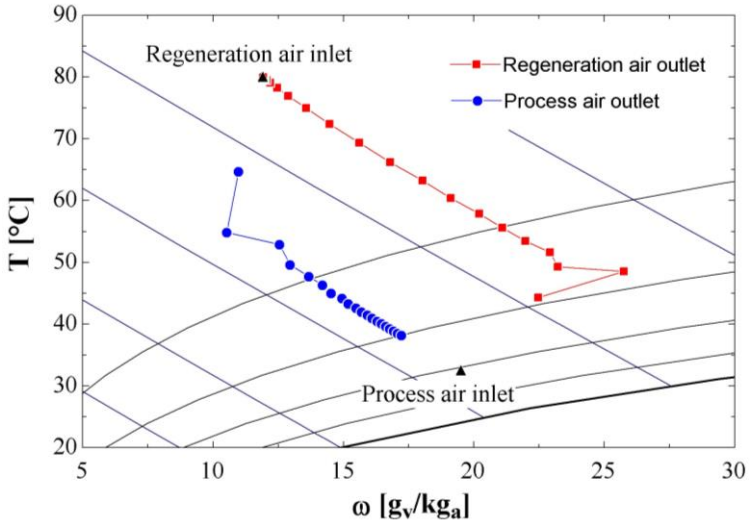

Figure 7. Computed air outlet conditions for the reference case with *N*=20 rph

From Fig. 7 it is observed that the air outlet conditions fluctuate in the first circumferential control volumes of both DW sections before stabilizing along almost isenthalpic lines. The fluctuations do not have physical meaning, but they depend on the model implementation.
To better understand the model behavior, the air and desiccant temperature and water content distributions along the circumferential and axial directions are shown in Fig. 8 for the reference case.

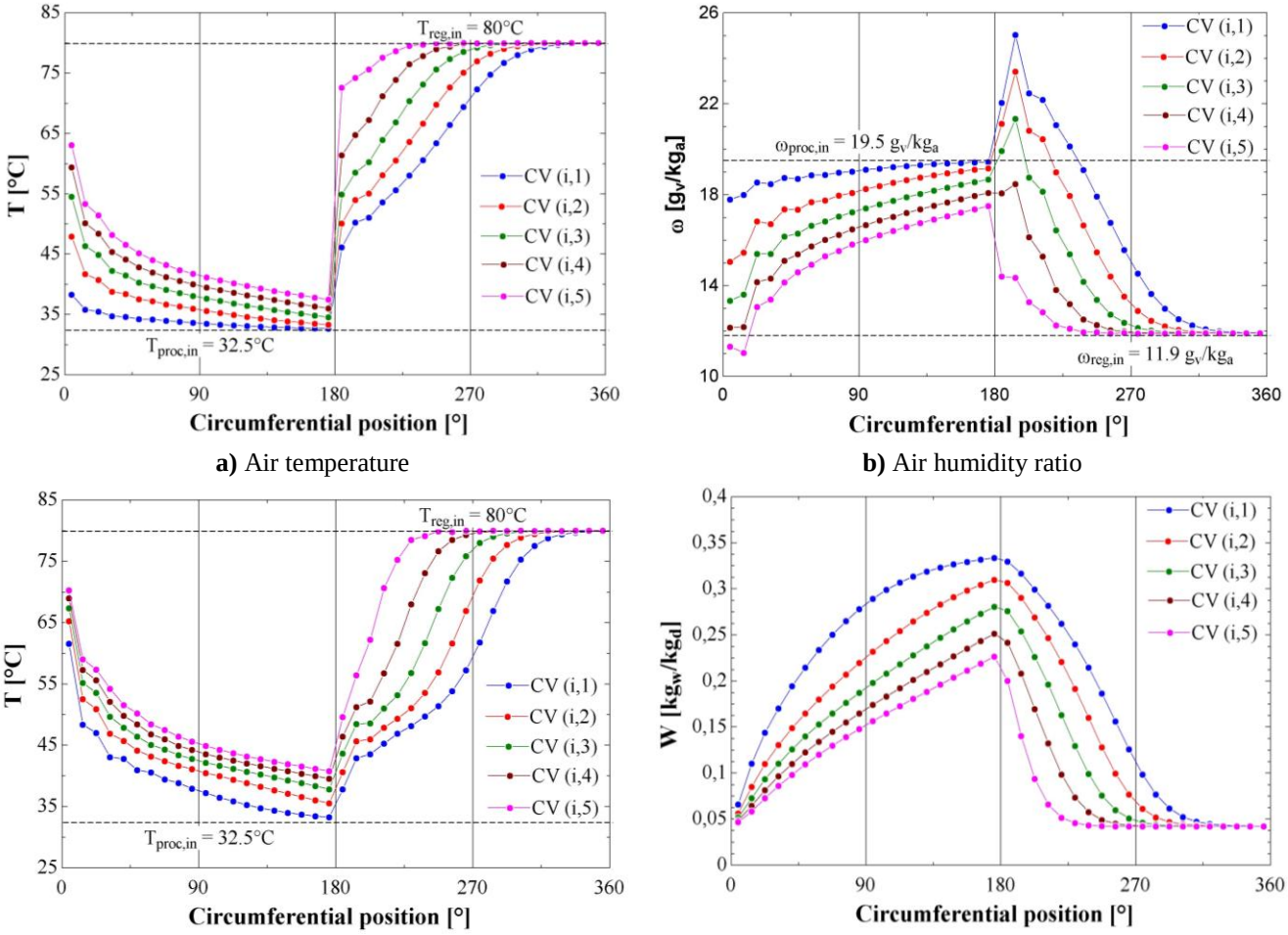

a) Air temperature

b) Air humidity ratio

c) Desiccant temperature

d) Desiccant water content

Figure 8. Compute temperatures and water content distributions for the reference case with *N*=20 rph

In Fig. 8 the fluctuations are visible in the first circumferential control volumes at both DW sections for all axial control volumes. At these locations the air and desiccant conditions have the steepest change. However the distributions along the axial direction look reasonable. It is also noticed that, at the end of the regeneration side (circumferential position between approx. 320° and 360°), the air and desiccant conditions do not change both axially and circumferentially, i.e. air and desiccant are in equilibrium and no more water can be desorbed with the specified regeneration air inlet conditions.

4. DISCUSSION

Before discussing the results it shall be remembered that the considered experimental data are taken from (Tsutsui, 2008) and not gathered during this study. More experimental data are necessary to validate the model for varying air inlet conditions at both wheel sides and different regeneration angles.

In addition, the observed fluctuations from Fig. 7 and 8 can influence the results to some extent, making more difficult to identify the physical causes of improper behaviors of the model. Fluctuations can be reduced or eliminated by applying higher order schemes and/or by rewriting the sensible heat transfer in Eq. (6) using a more accurate air-desiccant temperature difference definition (e.g. logarithmic mean temperature difference), in both cases increasing the computational time.

The comparison with experimental data shows that the model reproduces the overall physical behavior of DWs. Dehumidification is strongly influenced by the difference in water vapor concentration between the bulk air and the desiccant surface and weakly influenced by the convective mass transfer resistance, since varying the exponent *n* in Eq. (14) does not affect the results much. The model seems to underestimate the heating effect on the process airstream, and to both underestimate and overestimate the dehumidification effect depending on the wheel rotational speed. A possible cause is the model does not consider the solid-side mass diffusion resistance: diffusion phenomena in the desiccant pores (surface diffusion, Knudsen diffusion, multilayer adsorption, etc.) are already found to limit adsorption and desorption rates from previous studies (Pesaran and Mills, 1987), (Goldsworthy and White, 2012). The dimensionless Biot number is a useful indicator to measure the relative magnitude of the resistance to heat or mass transfer from the humid air to the solid as compared to the resistance to heat or mass transfer within the solid itself. Biot numbers much lower than 1 indicate the gas-side resistance dominates over the solid-side resistance, and vice versa. As reported in (Goldsworthy and White, 2014), common desiccant wheels have Biot numbers for heat transfer much lower than 1 and for mass transfer in the order of 10, as it is for the wheel considered in this study, i.e. "*both the solid-side and gas-side resistances are potentially important for moisture transport*". The mass diffusion rate in the solid is influenced by the rotational speed: higher rotational speeds imply shorter contact times between air and desiccant, i.e. lower mass transfer rates. Implementing the solid-side mass transfer resistance in steady state simulations requires an expression for the water concentration profile in the desiccant as a function of the influencing parameters (e.g. rotational speed).

The computational effort to solve the model is low: no more than 10 s are needed for a complete simulation. This makes the model particularly suitable for complete HVAC system simulations and optimizations.

The actual version of the model differs from the models presented in (Tsutsui, 2008) and (Harshe et al., 2005) because the convective heat and mass transfer coefficients are calculated for each control volume and not kept constant, hence entrance effects are taken into account. In both (Tsutsui, 2008) and (Harshe et al., 2005) mass transfer in the solid is not implemented. In (Harshe et al., 2005) it is proposed to fit experimental data by means of constant tuning parameters for Nusselt and Sherwood numbers, which cannot precisely describe phenomena varying with operational conditions (e.g. solid-side mass diffusion).

5. CONCLUSIONS

A steady state 2D model of desiccant wheels has been built and validated against experimental data from the literature. The model reproduces the same trends shown by experimental data for the considered varying parameters. Some underestimation and overestimations of the performances still occur. Possible causes are the lack of more precise experimental data for this study, some minor computational errors leading to fluctuations of the air and desiccant conditions along the circumferential direction, and the absence of any mass diffusion resistance in the solid. Water diffusion in the desiccant pores plays an important role in the adsorption and desorption processes, and should be considered in a future version of the model. More detailed experiments have to be carried out to check and correct the discrepancies and further validate the model for all possible input variations. The low computational effort required by the model makes it particularly suitable for complete system simulations, where computational times can be discriminant. Moreover the flexibility of the model in terms of inputs allows for optimization of desiccant wheels as well as entire systems.

NOMENCLATURE

A	apparent desiccant area	(m^2)
a	channel height	(m)
b	channel width	(m)
c	channel wall thickness	(m)
c_p	specific heat capacity	(J/kgK)
D_h	channel hydraulic diameter	(m)

Subscripts

a	dry air
d	dry desiccant
eq	equilibrium
ha	humid air
m	solid matrix

h	heat transfer coefficient	(W/m^2K)	v	water vapor
I	specific enthalpy	(J/kg)	w	water
L	wheel length	(m)	wm	wet solid matrix
Le	Lewis number	(-)		
N	wheel rotational speed	(rph)		
Nu	Nusselt number	(-)		
$\dot{m}$	mass flow rate	(kg/s)		
Pr	Prandtl number	(-)		
$\dot{Q}$	heat flow rate	(W)		
q_{ads}	heat of adorption	(J/kg)		
q_{vap}	latent heat of vaporization	(J/kg)		
Re	Reynolds number	(-)		
T	temperature	(°C)		
u	velocity	(m/s)		
W	desiccant water content	(g_w/kg_d)		
σ	mass transfer coefficient	(kg/m^2s)		
ω	humidity ratio	(kg_v/kg_a)		

REFERENCES

Barlow, R.S., 1982, Analysis of the Adsorption Process and of Desiccant Cooling Systems: A Pseudo-steady-state Model for Coupled Heat and Mass Transfer. Solar Energy Research Institute.

Brandemuehl, M.J., 1982, Analysis of Heat and Mass Regenerators with Time Varying or Spatially Nonuniform Inlet Conditions, PhD Thesis, Department of Mechanical Engineering, University of Wisconsin.

De Antonellis, S., Joppolo, C.M. and Molinaroli, L., 2010, Simulation, performance analysis and optimization of desiccant wheels, *Energy and Buildings*, 42, 9: 1386-1393.

Ge, T.S., Li, Y., Wang, R.Z. and Dai, Y.J., 2008, A review of the mathematical models for predicting rotary desiccant wheel. *Renewable & Sustainable Energy Reviews*, 12, 6: 1485-1528.

Goldsworthy, M., White, S.D., 2014, The Performance of Desiccant Wheels for Desiccant Air-Conditioning, *In*: Nóbrega, C.E.L., Brum, N.C.L., *Desiccant-Assisted Cooling*, Springer London: 109-141.

Goldsworthy, M., White, S.D., 2012, Limiting performance mechanisms in desiccant wheel dehumidification. *Applied Thermal Engineering*, 44: 21-28.

Harshe, Y., Utikar, R., Ranade, V. and Pahwa, D., 2005, Modeling of rotary desiccant wheel, *Chemical Engineering& technology*, 28, 12: 1473-1479.

La, D., Dai, Y.J., Li, Y., Wang, R.Z. and GE, T.S., 2010, Technical development of rotary desiccant dehumidification and air conditioning: A review. *Renewable & Sustainable Energy Reviews,* 14, 1: 130-147.

Mills, A.F., 2001, *Mass Transfer*. Prentice Hall PTR.

Pesaran, A.A., 1980, Air Dehumidification in Packed Silica Gel Beds, M.S. Thesis, School of Engineering and Applied Science, University of California Los Angeles.

Pesaran, A.A., Mills, A.F., 1987, Moisture transport in silica gel packed beds-I.Theoretical study. *International Journal of Heat and Mass Transfer*, 30, 6: 1037-1049.

Tsutsui, K., 2008, Effect of design and operating conditions on performance of desiccant wheels. *IIR 2008 HVAC energy efficiency best practice conference*, Melbourne.